Rubber/LDH Nanocomposites by Solution Blending

T. Kuila,[1] S. K. Srivastava,[1] A. K. Bhowmick[2]

[1]*Department of Chemistry, Inorganic Materials and Nanocomposite Laboratory, Indian Institute of Technology, Kharagpur 721302, India*
[2]*Rubber Technology Centre, Indian Institute of Technology, Kharagpur 721302, India*

Received 2 April 2008; accepted 18 August 2008
DOI 10.1002/app.29117
Published online 12 October 2008 in Wiley InterScience (www.interscience.wiley.com).

ABSTRACT: The rubber nanocomposites containing ethylene vinyl acetate (EVA) having 60 wt % of vinyl acetate content and organomodified layered double hydroxide (DS-LDH) as nanofiller have been prepared by solution intercalation method and characterized. The XRD and TEM analysis demonstrate the formation of completely exfoliated EVA/DS-LDH nanocomposites for 1 wt % filler loading followed by partially exfoliated structure for 5–8 wt % of DS-LDH content. EVA/DS-LDH nanocomposites show improved mechanical properties such as tensile strength (TS) and elongation at break (EB) in comparison with neat EVA. The maximum value of TS (5.1 MPa) is noted for 3 wt % of DS-LDH content with respect to TS value of pure EVA (2.6 MPa). The data from thermogravimetric analysis show the improvement in thermal stability of the nanocomposites by ≈15°C with respect to neat EVA. Limiting oxygen index measurements show that the nanocomposites act as good flame retardant materials. Swelling property analysis shows improved solvent resistance behavior of the nanocomposites (1, 3, and 5 wt % DS-LDH content) compared with neat EVA-60. © 2008 Wiley Periodicals, Inc. J Appl Polym Sci 111: 635–641, 2009

Key words: EVA-60; layered double hydroxide; nanocomposites; mechanical; TGA; LOI; swelling

INTRODUCTION

Recently, polymer/layered double hydroxide (LDH) nanocomposites have been studied extensively for their remarkable improvement in the mechanical properties, thermal stability, reduced gas permeability, and flame retardancy compared with virgin polymers and traditional organic–inorganic composites.[1–5] This is mainly due to the effective dispersion of LDH layers of nanometer thickness with the aspect ratios of about 30–100 within the polymer matrix.[1,6] In most of the cases, LDH layers are dispersed homogeneously in the polymer matrix inducing strong interfacial interaction with the polymer matrix.[1] The lamellar structure and anion exchange properties of LDHs make them attractive for technological application such as ion-exchangers, adsorbent materials, pharmaceutical stabilizers, and precursors for new catalytic materials.[7] The endothermic decomposition of LDH produces sufficient water vapor and metal oxide residue which impedes the burning process by reducing the oxygen supply to the bulk phase. The LDH can be modified by the replacement of interlayer anions such as Cl^-, NO_3^-, or CO_3^{2-} with organic anionic surfactant, such as sodium dodecyl sulfate (SDS), sodium dodecyl benzene sulfonate (SDBS) increasing thereby the gallery height of such organically modified LDH.[1,3] The expected structural diagram of pure LDH to dodecyl sulfate (DS) intercalated LDH (DS-LDH) is shown in Figure 1.

LDH nanocomposites with various polymers such as polyimide,[3] poly(ethylene terephthalate) (PET),[5,8] high-density polyethylene (HDPE),[9] polystyrene,[10] ethylene–propylene–diene monomer (EPDM),[1] ethylene vinyl acetate (EVA),[11,12] poly(propylene carbonate),[13] and poly(vinyl chloride) (PVC),[14] concerning physical properties and dispersion, have been widely reported. EVA copolymer is one of the most important organic polymers, extensively used for the application of electrical insulation, cable jacketing and repair, component encapsulation, water proofing, corrosion protection, and component packaging. However, bulk EVA does not fulfill the requirements in terms of thermal stability and mechanical properties in some specific areas, e.g., hosepipes and cables, therefore, many nanofillers such as organomodified clay especially montmorillonite (MMT),[15–19] nanomagnesium hydroxide [$Mg(OH)_2$][20] have been used to prepare nanocomposites of EVA to investigate the improvements in their properties. Our previous reports show that the nanocomposites of EVA-18, 28, and 45 with DS-LDH possess higher mechanical and thermal properties.[11,12] EVA-60 is another

Correspondence to: S. K. Srivastava (sunit@chem.iitkgp.ernet.in).
Contract grant sponsor: CSIR, New Delhi, India.

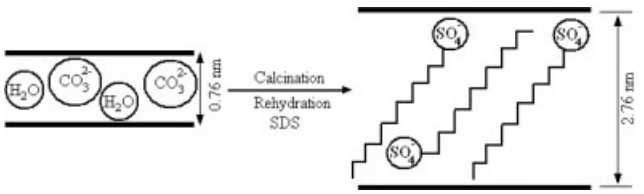

Figure 1 Schematic diagram of pure LDH and DS-LDH.

polymer which is highly rubbery in nature. It is very soft and pliable, having high content of vinyl acetate (VA) which facilitates superior interaction between VA and DS-LDH. Therefore, the present work is focused on developing EVA-60 nanocomposites using organomodified Mg-Al LDH (DS-LDH) to study the effect of filler loading on its mechanical, thermal, and flame-retardant properties.

EXPERIMENTAL

Materials

EVA copolymer with 60 wt % of vinyl acetate content was supplied by LANXESS Europe GmbH (Langenfeld, Germany) (Levamelt 600; melt flow index = 2.75 ± 1.25 g/10 min) and the crosslinking agent dicumyl peroxide (DCP) (DiCUP-98, from Hercules, USA) was used to prepare the pristine EVA and EVA/DS-LDH nanocomposites. $Mg(NO_3)_2 \cdot 6H_2O$, $Al(NO_3)_3 \cdot 9H_2O$, and Na_2CO_3 were purchased from E. Merck (Mumbai, India). Sodium hydroxide (Quest Chemicals, Kolkata, India) and sodium dodecyl sulfate (SRL Pvt., Mumbai, India) were used to prepare DS intercalated layered double hydroxide. Toluene and Xylene were used as solvent and purchased from SRL, Mumbai, India.

Preparative method

The Mg-Al LDH and organomodified LDH (DS-LDH) used here have been synthesized according to our previously reported method.[12] In the preparation of EVA/DS-LDH nanocomposites, only EVA (EVA-18, 28, 45) has been replaced by EVA-60 retaining all other conditions are analogous to the earlier methods.[11,12]

Characterization

The interlayer spacing of DS-LDH before and after intercalation by polymer chains were investigated by X-ray diffraction (XRD) analysis, using a PANalytical (PW 3040/60), "X" Pert Pro with Cu K_α radiation ($\lambda = 1.541$ Å) at a generator current of 100 mA, scanning over the 2θ range from 2° to 10° at a scanning rate of 2°/min. Nanoscale dispersion of DS-LDH in EVA matrix were analyzed using a JEOL 2100 200 kV transmission electron microscope (TEM). The tensile properties were recorded on a Zwick/Roell Z010 at a strain rate of 100 mm/min at 25 ± 2°C. Thermogravimetric analysis of the neat polymer and the nanocomposites were carried out on Redcroft 870 thermal analyzer, Perkin-Elmer with a heating rate of 10°C/min over a temperature range of 60 to 600°C in air. The initial weight taken for this analysis was ~ 5 mg for each sample. Isothermal TGA was performed with Redcroft 870 thermal analyzer, Perkin–Elmer by heating the sample at 300°C for 3 h in nitrogen atmosphere. The flame-retardancy test of all the samples was carried out by the measurement of limiting oxygen index (LOI) value by the flammability tester (S.C. Dey Co., Kolkata) as per the standard ASTM D 2863-77. The solvent uptake capacity (Xylene, 25°C) and crosslink density (number of active network chain segments per unit volume) were determined on the basis of rapid solvent swelling measurement by the application of Flory-Rehner equation.[21] The gravimetric method (ASTM D 2765-95, Method C) were followed for swelling measurements.

RESULTS AND DISCUSSION

XRD analysis

Figure 2 displays the XRD patterns of DS-LDH and the nanocomposites of EVA with 1–8 wt % of DS-LDH contents. It is observed that the pure DS-LDH shows a peak at 2θ ≈ 3.2° equivalent to an interlayer distance of 2.76 nm. However, no such diffraction

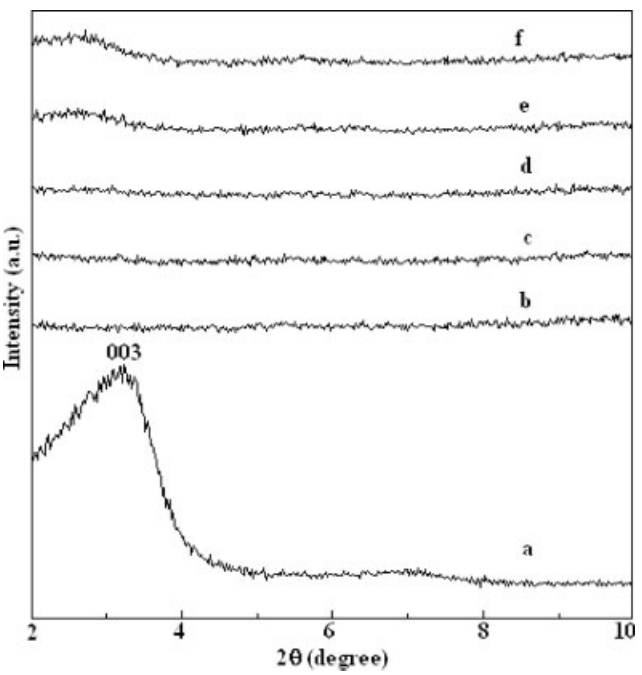

Figure 2 XRD spectra of (a) DS-LDH, (b) EVA-60, and (c) EVA-60/DS-LDH (1 wt %), (d) EVA-60/DS-LDH (3 wt %), (e) EVA-60/DS-LDH (5 wt %), (f) EVA-60/DS-LDH (8 wt %) nanocomposites.

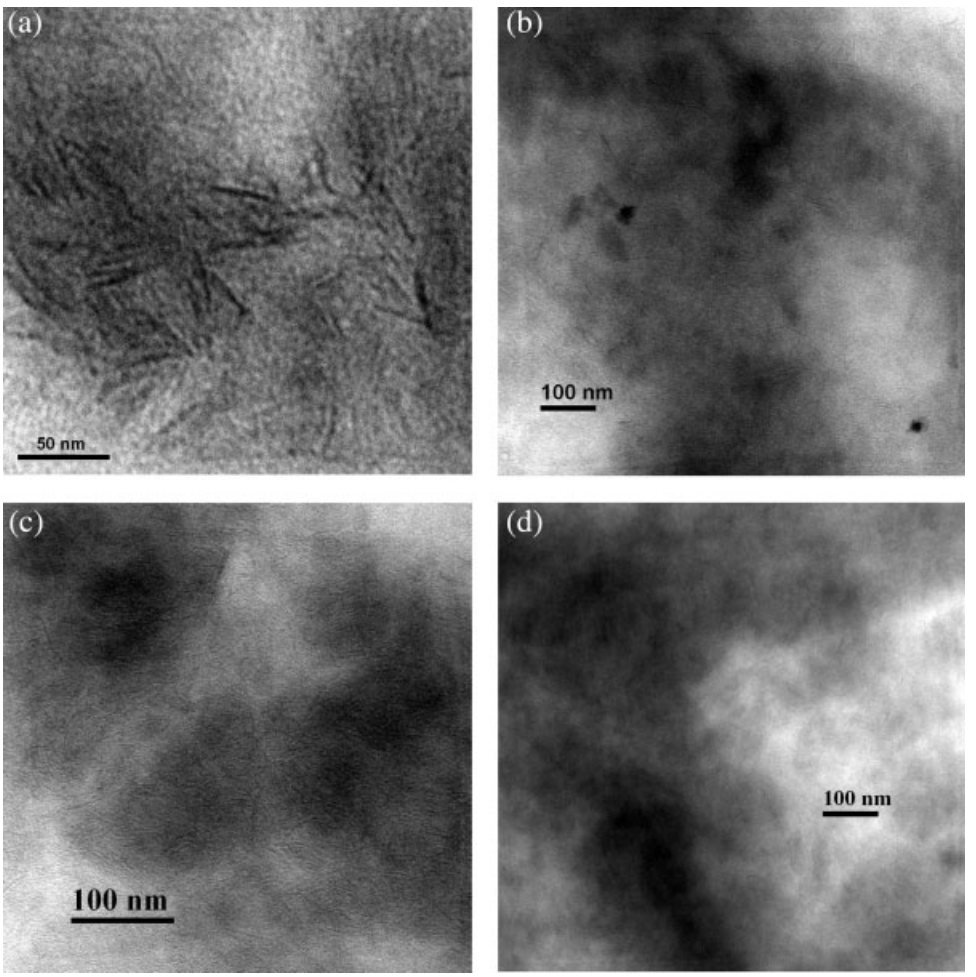

Figure 3 TEM images of (a) fully exfoliated EVA-60/DS-LDH (1 wt %) nanocomposite, (b) partially exfoliated EVA-60/DS-LDH (3 wt %) nanocomposite, (c) partially exfoliated EVA-60/DS-LDH (5 wt %) nanocomposites, and (d) aggregated morphology of EVA-60/DS-LDH (8 wt %) nanocomposite.

peak is noted in case of the nanocomposites with 1 and 3 wt % DS-LDH contents. This observation clearly demonstrates the destruction of ordered layer structure of DS-LDH when EVA-60 molecular chains intercalate between the interlayer space of DS-LDH and exfoliated structure has formed during intercalation. This has been further confirmed by transmission electron microscopy (TEM) observation. A smooth shoulder is visible in 5 wt % DS-LDH loading, indicating the formation of partially exfoliated/intercalated morphology.[22,23] However, for the nanocomposites containing 8 wt % DS-LDH, a broad diffraction peak appears at $2\theta \approx 2.5^\circ$ in the diffractogram indicating the possibility of partially exfoliated nanocomposite structure.[1,22,23]

TEM analysis

The TEM images of the EVA nanocomposites with different amount of DS-LDH content (1, 3, 5, and 8 wt %) are presented in Figure 3(a–d). The bright field represents the EVA matrix whereas the dark lines refer to the LDH layers. The TEM image of the nanocomposite with 1 wt % filler loading [Fig. 3(a)] shows the presence of delaminated DS-LDH layers throughout the polymer matrix. The thickness and lateral dimension of the exfoliated LDH layers corresponds to 6–8 nm and 30–40 nm, respectively. On the contrary, for 3 and 5 wt % of DS-LDH content in EVA, the distribution of filler is relatively less homogeneous [Fig. 3(b,c)]. It is also evident from TEM image that some parts of DS-LDH nanolayers are intercalated while most of these are exfoliated to form intercalated–exfoliated structure. However, the TEM image [Figure 3(d)] for 8 wt % DS-LDH content shows that the DS-LDH nanolayers are not only intercalated but also aggregated in the EVA matrix.

Mechanical properties

To evaluate the reinforcing effect of DS-LDH into the EVA matrix, mechanical properties during extension are measured. Figure 4 shows the variation of tensile strength (TS) and elongation at break (EB)

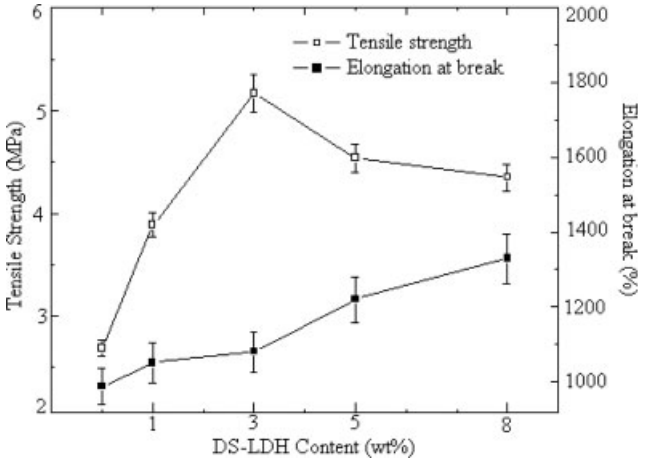

Figure 4 Variation of tensile strength and elongation at break with 0, 1, 3, 5, and 8 wt % DS-LDH contents in EVA-60 matrix.

with DS-LDH. According to this, TS for the nanocomposites is superior with respect to neat EVA and it is highest for 3 wt % of DS-LDH content. Because of high surface area of DS-LDH nanoparticles in EVA matrix, the applied stress is expected to transfer from matrix onto the DS-LDH particles resulting in the enhancement of mechanical properties.[24] A polar interaction between the hydroxyl group of LDH and the acetate group of EVA through hydrogen bonding is also favorable for the enhancement of mechanical properties.[11] At higher filler loading (5 and 8 wt %), gradual decrease in TS is observed, though in either case the TS values are higher compared with neat EVA. Such reduction in TS is associated with the extended aggregation of DS-LDH layers, and which increases with increasing the DS-LDH content in EVA. These findings are in good agreement with the similar deterioration of mechanical properties reported on polyimide/LDH nanocomposites.[3] It is also evident from Figure 4 that the addition of DS-LDH in EVA results in increase in the elongation at break (EB) and is at a maximum for 3 wt % DS-LDH in EVA. The improvement in EB may be due to the extensive entanglement of the crosslinkable polymer chains and synergistic effect of platelet orientation and chain slippage.[25] Figure 5 plots the stress–strain curves of neat EVA and its nanocomposite with varying amount of DS-LDH contents. It shows that the tensile moduli at different elongation percents are relatively higher for the nanocomposites containing 1, 3, and 5 wt % DS-LDH, compared with neat EVA. The enhanced tensile moduli for these nanocomposites correspond to the formation of some shear zones when the nanocomposites are under stress and strain conditions.[26] Such an improvement in mechanical properties can also be accounted on the basis of static adhesion strength as well as interfacial stiffness because of the efficient stress transfer at the interface originating elastic deformation from the large aspect ratio of the nanofiller.[25] On further addition of DS-LDH, the tensile modulus is decreased possibly due to aggregation of DS-LDH nanolayers.

TGA analysis

The thermal degradation behaviors of the nanocomposites in air have been monitored by TGA. Figure 6 shows the thermogravimetric curves of pure EVA and its nanocomposites with DS-LDH. It is seen that the TG curves of neat EVA and the nanocomposites show three main steps due to the weight loss.[27] The weight loss for the first step in all the nanocomposites is mainly attributed to the early degradation of alkyl chains of organomodified LDH.[28] The second weight loss (304°C to 435°C) of neat EVA and EVA/DS-LDH nanocomposites is mainly ascribed to the deacylation of acetate functionality. It is also noted that the onset decomposition temperature for this step remains more or less same for all the nanocomposites, and is accompanied by the decrease in % weight loss corresponding to this temperature. This is probably due to the excellent barrier effect of homogeneously dispersed DS-LDH nanolayers, as evident from the TEM images [Fig. 3(a–c)]. The third step weight loss (519°C to 534°C) in thermogram shows that the final decomposition temperature is ≈13–15°C higher for the nanocomposites compared to neat EVA. At this stage of degradation, the weight loss is significantly decreased with the gradual addition of DS-LDH. It appears that at the early stage of the decomposition, the char formation takes place at the surface of the nanocomposites. It prevents the

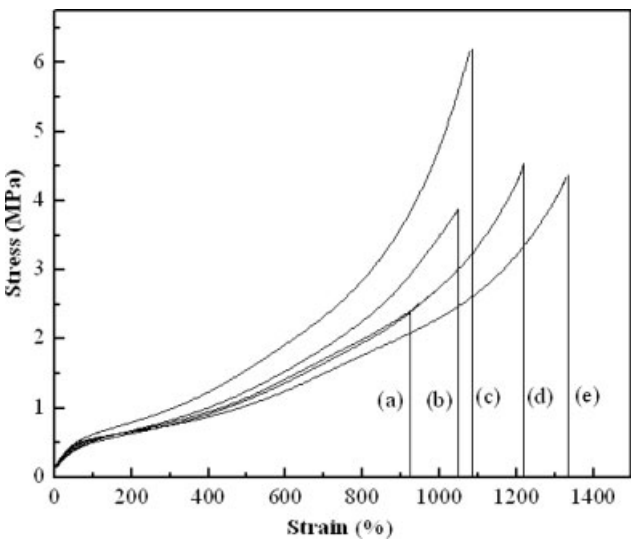

Figure 5 Stress versus strain plot of (a) pure EVA-60, (b) EVA-60/DS-LDH (1 wt %), (c) EVA-60/DS-LDH (3 wt %), (d) EVA-60/DS-LDH (5 wt %), (e) EVA-60/DS-LDH (8 wt %) nanocomposites.

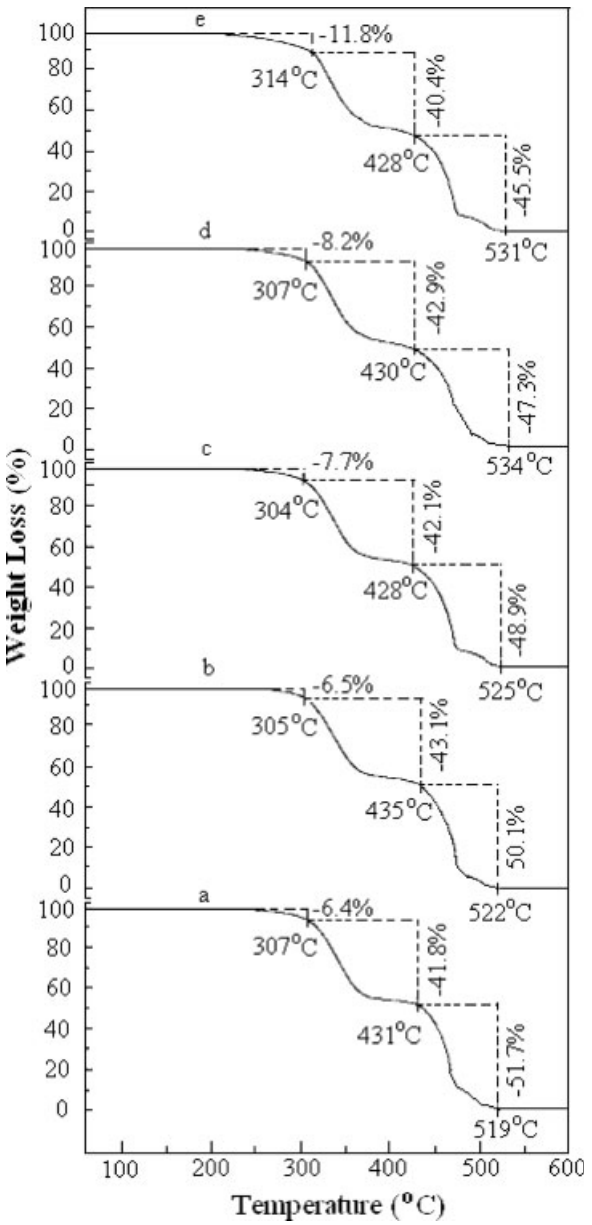

Figure 6 TGA profiles of EVA-60/DS-LDH nanocomposites with (a) 0, (b) 1, (c) 3, (d) 5, and (e) 8 wt % DS-LDH content.

emission of thermally degraded small gaseous molecules through the charred layer enhancing thereby the thermal decomposition temperature of the nanocomposites.[29]

Figure 7 represents the plots of the isothermal degradation curves for EVA/DS-LDH nanocomposites held at 300°C for 3 h. According to this, thermal degradation of these nanocomposites occurs more slowly than pure EVA. The initial decomposition of neat EVA is accompanied by the deacylation of acetate functionality. Figure 7 also shows that the thermal stability of the nanocomposites (1–5 wt %) are much higher compared with pure EVA. However, for 8 wt % filler loading, thermal stability of the nanocomposites decreases slightly, but remains higher with respect to neat EVA. Such a behavior is probably associated with the morphological changes in relative proportion of exfoliated and intercalated species with the DS-LDH loading. At lower filler loading (1 wt %), exfoliation dominates, whereas the amount of exfoliated nanolayer is not enough to enhance the thermal stability of the EVA nanocomposite. When DS-LDH concentration is increased to 3 and 5 wt %, relatively more exfoliated layers are formed thereby leading to excellent barrier effect and so higher thermal stability. At higher filler loading (8 wt %), the formation of aggregated DS-LDH layers dominates which probably does not allow to maintain good thermal stability. The DS-LDH layers act as heat accumulators offering an extra heat source to polymer degradation.[30,31] Hence, at loadings higher than that required for the maximum barrier effect, the filler particles performing as heat accumulators start to decrease polymer's thermal stability. These observations clearly reaffirm our contention that the DS-LDH nanolayers act as excellent barrier in EVA/DS-LDH nanocomposites.

Limiting oxygen index

Figure 8 represents the findings on limiting oxygen index (LOI) of neat EVA and its nanocomposites. It is observed that burning of pure EVA takes place very rapidly in comparison to its corresponding nanocomposites. The calculation shows that the LOI values are relatively higher for the nanocomposites than neat EVA (19.3). The maximum value of LOI (24.8) is noted for 8 wt % DS-LDH content in EVA. This is mainly attributed to the presence of char layer in the nanocomposites which impedes burning while acting as a barrier between the burning

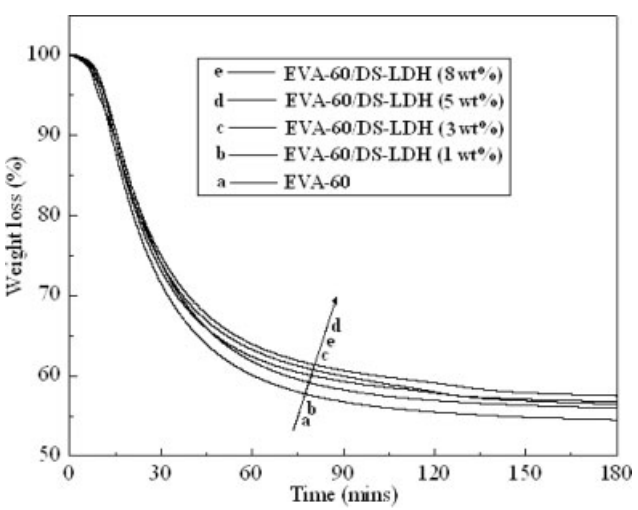

Figure 7 Isothermal TGA curves of EVA-60/DS-LDH nanocomposites with various amount of DS-LDH contents at 300°C for 3 h.

surface and supplied oxygen.[20] For the nanocomposites with DS-LDH content of $\leq$ 3 wt %, the thickness of char layer appears to be very thin and may not be thick enough to prevent burning of the composites. However, beyond 3 wt % of DS-LDH loading, formation of thick char layer is likely to suppress the propagating downward flame by disrupting oxygen supply to the burning specimen.[29] In addition, the endothermic decomposition of LDH produces sufficient smoke and water vapor which also accounts for the reduction of flammable characteristics in the case of nanocomposites.[32]

Crosslinking density by swelling

The effect of DS-LDH in EVA on the solvent (xylene) uptake characteristics and crosslink density is displayed in Figure 9. It shows that the solvent uptake ability of the nanocomposites decreases whereas the crosslinking density in the swollen gel increases for, up to 3 wt % of DS-LDH content in EVA, in comparison with its pure counterparts. This clearly suggests that the strong interfacial interaction between the polymer chains and DS-LDH layers inhibit the penetration of xylene molecules from surface to bulk region of the nanocomposites thereby reducing the uptake of xylene.[33] An increase in crosslink density would result in increased modulus which have been discussed earlier in Figure 5. It shows that the mechanical data correlates well with the crosslink density.

At higher DS-LDH contents in EVA, a reverse trend in the solvent uptake and crosslink density is observed. Such behavior can be attributed to the common adsorption tendency of peroxide on filler surfaces,[34,35] according to which the concentration of peroxide available for crosslinking of EVA is reduced. As a result, the available vacant sites in polymer matrix are increased which accounts for the increase in the solvent uptake during swelling.[35–38] However, the observed decrease in crosslinking density may be attributed to the increase in exfoliated dispersion in the nanocomposites.[39]

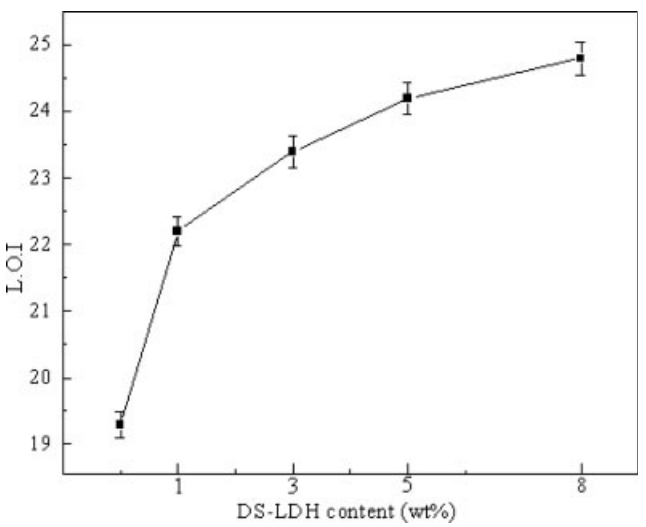

Figure 8 Effect of DS-LDH content on the LOI values of EVA-60/DS-LDH nanocomposites.

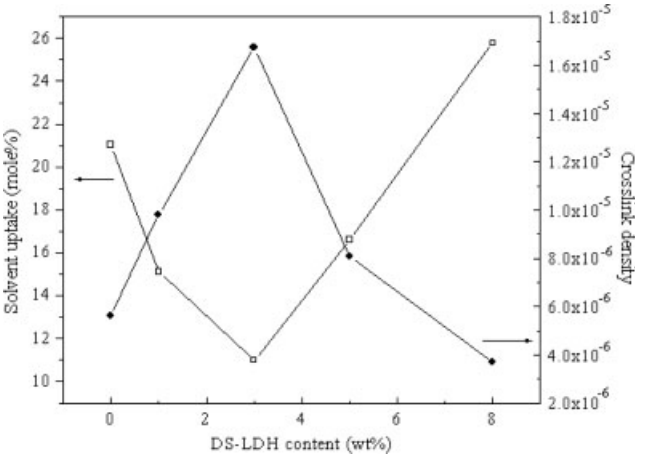

Figure 9 Influence of DS-LDH content on the xylene uptake (mole %) and crosslinking density for EVA-60 nanocomposites.

CONCLUSIONS

EVA/DS-LDH nanocomposites have been synthesized successfully by solution intercalation method. XRD and TEM analysis clearly demonstrate that at 1 wt % and 3–8 wt % of DS-LDH loadings, the exfoliated and partially exfoliated nanocomposites are formed, respectively. Mechanical properties of the nanocomposites are much higher compared with neat EVA with an optimum value of TS for 3 wt % DS-LDH content in EVA. Thermal stability of the EVA/DS-LDH nanocomposites is increased by about 12–15°C compared with neat EVA. Determination of LOI values of the nanocomposites show the improved flame retardant characteristics. The solvent resistance property of the nanocomposites is improved at low filler loading.

Authors are also thankful to LANXESS Europe GmbH, Langenfeld, Germany, for providing the EVA for this work.

References

1. Acharya, H.; Srivastava, S. K.; Bhowmick, A. K. Compos Sci Technol 2007, 67, 2807.
2. Costa, F. R.; Satapathy, B. K.; Wagenknecht, U.; Weidisch, R.; Heinrich, G. Euro Polym J 2006, 42, 2140.
3. Hsueh, H. B.; Chen, C. Y. Polymer 2003, 44, 1151.
4. Camino, C.; Maffezzoli, A.; Braglia, M.; Lazzaro, M. D.; Zammarano, M. Polym Degrad Stab 2001, 74, 457.

5. Lee, W. D.; Im, S. S. J Polym Sci Part B: Polym Phys 2007, 45, 28.
6. Tao, Q.; Zhang, Y.; Zhang, X.; Yuan, P.; He, H. J Solid State Chem 2006, 179, 708.
7. Wu, G.; Wang, L.; Evans, D. G.; Duan, X Eur J Inorg Chem 2006, 2006, 3185.
8. Lee, W. D.; Im, S. S.; Lim, H. M.; Kim, K. J Polym 2006, 47, 1364.
9. Ding, P.; Qu, B. J Polym Sci Part B: Polym Phys 2006, 44, 3165.
10. Ding, P.; Qu, B. J Appl Polym Sci 2006, 101, 3758.
11. Kuila, T.; Acharya, H.; Srivastava, S. K.; Bhowmick, A. K. J Appl Polym Sci 2007, 104, 1845.
12. Kuila, T.; Acharya, H.; Srivastava, S. K.; Bhowmick, A. K. J Appl Polym Sci 2008, 108, 1329.
13. Du, L.; Qu, B.; Meng, Y.; Zhu, Q. Compos Sci Technol 2006, 66, 913.
14. Bao, Y. Z.; Huang, Z. M.; Weng, Z. X. J Appl Polym Sci 2006, 102, 1471.
15. Alexandre, M.; Dubonis, P. Mater Sci Eng R 2000, 28, 1.
16. Pramanik, M.; Srivastava, S. K.; Samantaray, B. K.; Bhowmick, A. K. J Appl Polym Sci 2003, 87, 2216.
17. Srivastava, S. K.; Pramanik, M.; Acharya, H. J Polym Sci Part B: Polym Phys 2006, 44, 471.
18. Peeterbroeck, S.; Alexandre, M.; Jerome, R.; Dubois, P. Polym Degrad Stab 2005, 90, 288.
19. Alexandre, M.; Beyer, G.; Henrist, C.; Cloots, R.; Rulmont, A.; Jerome, R.; Dubois, P. Macromol Rapid Commun 2001, 22, 643.
20. Jiao, C. M.; Wang, Z. Z.; Ye, Z.; Hu, Y.; Fan, W. C. J Fire Sci 2006, 24, 47.
21. Mark, H. F.; Bikales, N.; Overberger, C. G.; Menges, G.; Kroschwitz, J. I. Encyclopedia of Polymer Science and Engineering, 2nd ed., vol. 4; Wiley: New York, 1990.
22. Liu, T.; Tjiu, W. C.; He, C.; Na, S. S.; Chung, T.-S. Polym Int 2004, 53, 392.
23. Liu, X.; Wu, Q.; Berglund, L. A.; Qi, Z. Macromol Mater Eng 2002, 287, 515.
24. Bikiaris, D. N.; Vassillou, A.; Pavlidou, E.; Karayannidis, G. Euro Polym J 2005, 41, 1965.
25. Acharya, H.; Srivastava, S. K.; Bhowmick, A. K. Polym Eng Sci 2006, 46, 837.
26. Acharya, H.; Pramanik, M.; Srivastava, S. K.; Bhowmick, A. K. J Appl Polym Sci 2004, 93, 2429.
27. Jiao, C.; Wang, Z.; Chen, X.; Yu, B.; Hu, Y. Radiation Phys Chem 2006, 75, 557.
28. Chen, W.; Feng, L.; Qu, B. Chem Mater 2004, 16, 368.
29. Costantino, U.; Gallipoli, A.; Nocchetti, M.; Camino, G.; Bellucci F.; Frache, A. Polym Degrad Stab 2005, 90, 586.
30. Kiliaris, P.; Papaspyrides, C. D.; Pfaendner, R. Macromol Mater Eng, to appear.
31. Ray, S. S.; Okamoto, M. Prog Polym Sci 2003, 28, 1539.
32. Costa, F. R.; Wagenknecht, U.; Heinrich, G. Polym Degrad Stab 2007, 92, 1813.
33. Burnside, S. D.; Giannelis, E. P. Chem Mater 1995, 7, 1597.
34. Chang, Y. W.; Yang, Y.; Ryu, S.; Nah, C. Polym Int 2002, 51, 319.
35. Song, M.; Wong, C. W.; Jin, J.; Ansarifar, A; Zhang, Z. Y.; Richardson, M. Polym Int 2002, 54, 560.
36. Patel, N. P.; Aberg, C. M.; Sanchez, A. M.; Capracotta, M. D.; Martin, J. D.; Sponta, R. J. Polymer 2004, 45, 5941.
37. Acharya, H.; Srivastava, S. K. Macromol Res 2006, 14, 132.
38. Maxwell, S. R.; Balazs, B. J Chem Phys 2002, 116, 10492.
39. Bharadwaj, R. K.; Mehrabi, A. R.; Hamilton, C.; Trujillo, C.; Murga, M.; Fan, R.; Chavira, A.; Thompson, A. K. Polymer 2002, 43, 3699.